Optics Communications 457 (2020) 124609

Contents lists available at ScienceDirect

Optics Communications

journal homepage: www.elsevier.com/locate/optcom

Nyquist four-level pulse amplitude modulation scheme (PAM-4) based on hierarchical modulation in IM/DD-TDM PON with hybrid equalization

Nan Feng [a,*], Xiang Sun [b]

[a] State Key Laboratory of Information Photonics and Optical Communications, Beijing University of Posts and Telecommunications, Beijing 100876, China

[b] Smart Edge Computing and Networking Lab., Department of Electrical and Computer Engineering, University of New Mexico, Albuquerque, NM 87131, USA

ARTICLE INFO

Keywords:
Intensity-modulation direct detection
Time division multiplexed passive optical network
Four-level pulse amplitude modulation
Hierarchical modulation
Nyquist pulse shaped
Equalization

ABSTRACT

In order to achieve higher power margin in the intensity-modulation and direct detection (IM/DD) based time division multiplexed passive optical network (TDM-PON) system, at the optical line terminal (OLT) side, we propose to use a Nyquist pulse shaped four-level pulse amplitude modulation (PAM-4) by using the electric low pass filter(LPF). In addition, we apply the hierarchical modulation (HM) scheme by assigning of most-significant bits (MSBs) and the less-significant bits (LSBs) of the PAM-4 symbol to optical network units (ONUs) located at different link positions. In addition, an overlap frequency domain equalizer (OFDE) and a vestigial-side band (VSB) filter are used to mitigate the linear inter symbol interference (ISI) and power fading (both of which are incurred by chromatic dispersion (CD)), respectively. The system performance, i.e., bit error rate (BER) and receiver sensitivity for both MSB and LSB, are analyzed by varying different system configurations. Simulation results show that increasing the hierarchical power ratio, which determines the significance difference between the points in the Nyquist pulse shaped HM PAM-4 constellation diagram, can increase the MSB's receiver sensitivity and reduce the LSB's receiver sensitivity. Furthermore, it has been demonstrated that the electric low pass filter can reduce the system ISI. In addition, the effect of linear ISI and power fading can be migrated by utilizing OFDE and VSB filter, respectively.

1. Introduction

The explosive growing network traffic introduces a significant bandwidth demand in a next-generation passive optical network (NG-PON) [1,2]. Due to low infrastructure cost, the intensity modulation and direct detection (IM/DD) based time division multiplexed PON (TDM-PON) system becomes a promising candidate for NG-PON [3,4]. With respect to advanced modulation formats applied in such IM/DD TDM-PON systems, four-level pulse amplitude modulation (PAM-4) can provide a higher spectral efficiency (SE) with low complexity as compared to the widely used ON-OFF keying (OOK) modulation [5–11]. Meanwhile, the Nyquist pulse shaped can be applied in an OLT to further improve SE by narrowing the spectrum of transmitting signals [12]. Therefore, the Nyquist pulse shaped multilevel PAM [13,14] format has been adopted in the IM/DD based TDM-PON system to achieve high SE and low cost. Based on that, Kikuchi et al. applied the Nyquist pulse shaped PAM-4 format [15] for short-range optical communications in the beyond 100G IM/DD system and experimentally verified its performance. In practical PON deployments, the actual link losses from an OLT to its ONUs are varied. For example, a longer distance between an OLT to an ONU incurs a lower signal to noise ratio (SNR), thus resulting in a lower power budget in the ONU, and vice versa. For example, an OLT is communicating with two ONUs, where the SNR between the OLT and ONU-1 is low, and thus OOK is applied to modulate and demodulate signals from the OLT to ONU-1. Meanwhile, in the conventional IM/DD based TDM-PON system, OOK should also be used to modulate and demodulate signals from the OLT to ONU-2 even though ONU-2 incurs much higher SNR and can adopt higher order modulations, such as PAM-4. Thus, the unused power budget forms the power margin. This essentially means that ONUs with higher SNR cannot fully utilize their power margin (i.e., their power margin is more than enough to accommodate low order modulation schemes). However, the power margin of the system is determined by the ONU with the worst SNR. In this case, if the redundant power margin can be utilized according to the actual channel conditions, the total power budget of the system can be improved. In order to fully utilize power margin, the hierarchical modulation (HM) technology [16,17] has drawn a lot of interests. Basically, HM allows different OLT-ONU links applies different modulation schemes based on their SNRs. That is, in the previous example, the link from the OLT to ONU-2 can

* Corresponding author.
E-mail addresses: fengnan@bupt.edu.cn (N. Feng), sunxiang@unm.edu (X. Sun).

[1] Receiver sensitivity of an ONU is defined as the minimum optical power received by the ONU such that the related bit error rate (BER) is no larger than the predefined threshold

https://doi.org/10.1016/j.optcom.2019.124609
Received 2 March 2019; Received in revised form 18 August 2019; Accepted 20 September 2019
Available online 23 September 2019

apply PAM-4 to modulate and demodulate the signals, thus improving the utilization of power margin for ONU-2. The HM technology has also been demonstrated to enhance the compatibility [18–21], network capacity [22–27], and flexibility [28–31] of the IM/DD based TDM-PON system. For example, authors in [18–21] employed HM in NG-PON to allow the legacy ONUs co-existence with the DSP based ONUs by constellation sharing. In addition, to increase the power budget of the total NG-PON, according to the SNR requirements of different links, the receiver sensitivity of ONUs[1] with higher path loss can be optimized by effectively redistributing power margin of the ONUs with lower loss. Santa et al. presented that the available power budget can be increased up to 3.5 dB with respect to a standard PAM-4 transmission in a 25 Gb/s TDM-PON system [23]. Similarly, Linden et al. proposed adaptive PAM modulation in PONs leveraging the distribution of optical path losses [24–27] to utilize the available network capacity with the given standard power budget. They also proposed the flexible non-uniform PAM for TDM-PON by allocating higher-order and lower-order modulation formats to the ONUs with and without enough optical power, respectively [28–31]. Moreover, it should be noted that, HM is a practical low cost solution of superposition coding (SC) [32,33] which has also been envisioned as a key technology in the power domain non-orthogonal multiple access (NOMA)-PON systems [34–38].

However, in the IM/DD based TDM-PON system, as the order of the modulation or baud rate increases, the receiver sensitivity of ONUs, which applies Nyquist pulse shaped PAM4 format [39–43], drops very rapidly because of linear inter symbol interference (ISI) and power fading (both of which are incurred by chromatic dispersion (CD)) [39,40]. Generally, the equalization methods include the optical equalization and digital equalization (which is implemented in a digital signal processing (DSP)). In order to mitigate linear ISI, different digital equalization methods can be applied [41–43]. Generally, the digital equalization can be achieved by implementing time-domain equalizer (TDE) and frequency domain equalizer (FDE). The essence of the both equalizer can be seen as a digital filter. For the TDE implementation, as the number of needed taps in equalizer, denoted as Nc, increases, the complexity of the TDE increases rapidly (i.e., O(Nc)). Thus, in order to reduce the complexity of the digital filter, instead of applying TDE, the FDE such as overlap frequency domain equalization (OFDE) whose complexity is (O(logNc)) [44–46], can be applied to achieve linear equalization. In addition, in order to reduce power fading in the IM/DD based TDM-PON system, the vestigial-side band (VSB) optical spectrum shaping technology can be considered an optical domain equalization method [47–50]. For instance, Liu et al. introduced the use of Nyquist PAM-4 at the OLT side to modulate the signal while the FDE and the VSB optical equalization were utilized to increase the ONU's receiver sensitivity [42]. In addition, Chen et al. compared the performance of transmitting PAM-4 and OOK modulated signals from an OLT to an ONU over 80 km standard single-mode fibers (SSMF) at a speed of 51.84-Gb/s, where a VSB filter is applied to mitigate the power fading [47].

Moreover, it has been demonstrated that applying HM in IM/DD based TDM-PON can improve the performance of the system However, it has not been investigated how much performance improvement can be achieved if we incorporating the Nyquist pulse shaped method and HM into IM/DD based TDM-PON system. Considering this as a primary motivation, in order to realize high power margin, and simple IM/DD-PON, this paper first investigate the HM scheme by containing two independent bit-streams with different significance in different layers. Then, we demonstrate the Nyquist shaped HM four-level PAM (HM-NPAM-4) format relying on an electric low pass filter (LPF) at the OLT side. Moreover, to further enhance transmission performance, this work mitigates the linear ISI effects and power fading effect by using the hybrid equalization which includes an applied digital domain OFDE and optical domain VSB filter. This paper mainly individually discusses the receiver sensitivity performance for 20G b/s transmission capabilities per wavelength HM-NPAM-4 by taking into consideration on different crucial system parameters. The simulation results show that there is a high correlation between the hierarchical power ratio and the SNR distribution in the IM/DD TDM-PON system. Furthermore, compared with the conventional PAM-4, the electric low pass filter can reduce the system ISI. In addition, the effect of linear ISI and power fading can be mitigated by utilizing OFDE and VSB filter, respectively

This paper is organized as follows. Section 2 presents the IM/DD based TDM-PON system, where HM-NPAM-4 is applied to modulate and demodulate the signals transmitted from an OLT to its ONUs. In Section 3, extensive simulations are conducted to evaluate the performance of IM/DD based TDM-PON by applying HM-NPAM-4. A brief conclusion is drawn in Section 4.

2. Applying HM-NPAM-4 in IM/DD based TDM-PON

The architecture of applying HM-NPAM-4 in IM/DD based TDM-PON is shown in Fig. 1. The signal is transmitted from an OLT to its ONUs via an ODN, which comprises a number of passive power splitters. Different ONUs may have different distance to the OLT, and thus the SNR values of the ONUs are also varied. Two ONUs with distinctive SNRs are paired to achieve HM-NPAM-4. For example, as shown in Fig. 1, ONU-1 and ONU-2 are paired, where ONU-1 has a lower SNR and ONU-2 has a higher SNR.

At the OLT side, the bit sequence (that are transmitted to ONU-1 and ONU-2) are firstly separated into two subsequences depending on the destination of the bits (i.e., whether bits are transmitted to ONU-1 or ONU-2) in the DSP part. The subsequence transmitted to ONU-1 and ONU-2 refers to as the most-significant bits (MSBs) and least-significant bits (LSBs), respectively. The two subsequences are then fed into a PAM-4 encoder (i.e., HM-PAM4 Mapping in Fig. 1), which encodes 2 bits (one from MSBs and the other from LSBs) into one symbol [51]. Fig. 2 shows the constellation diagram of HM-PAM-4 (i.e., PAM 2/4), where the hollow circles represent only fictitious symbols and the solid circles represent the actual transmitted symbols. Here,d_1 indicates the Euclidean distance between the constellation points in the fictitious PAM-2 (i.e., level-1 of hierarchy) constellation and d_2 indicates the Euclidean distance between the constellation points in the actual PAM-4 (i.e., level-2 of hierarchy) constellation. Denote γ as the hierarchical power ratio. Adjusting the value of γ can basically change d_1 and d_2. For example, the transmitted constellation for PAM-4 can be defined as $S = [-3, -1-2\gamma, 1+2\gamma, 3]$ [29]. Thus, $d_1 = 3+3\gamma$ and $d_2 = 2-2\gamma$. Hence, increasing γ essentially increases d_1 and reduces d_2, vice versa. Note that changing d_1 and d_2 may affect BER and receiver sensitivity of the ONUs. The amplitude of the generated HM-PAM-4 symbol is adjusted to form the optimal optical modulation index (OMI). Then the HM-PAM-4 signal is transmitted to digital-to-analog (DAC) and up-sampled by a factor of 2. Then an electric LPF is employed to perform Nyquist pulse shaping. Thus, the signal bandwidth is reduced by half [42]. Accordingly, the sampling rate of the required DAC /analog-to-digital converter (ADC) can be dropped.

Afterwards, the HM-NPAM-4 symbol is modulated based on the intensity of laser. The gradually-decreased spectrum occupies up to about a quarter of the double-side band (DSB) bandwidth. Then, the modulated optical signal is transmitted to a VSB filter, which is used to reduce power fading incurred by CD. The optical signal is then transmitted to an erbium-doped fiber amplifier (EDFA) via feeder fiber, where the EDFA is used to amplify the optical signal. The amplified optical signal is then transmitted to an optical band-pass filter, which is used to reduce the amplified spontaneous emission noise. After the optical splitter, different ONUs are placed after an additional distribution SSMF.

At the ONU side, the received optical signal is detected and converted into electrical signal based on a photo detector. The electrical signal is then transmitted to an offline DSP, which conducts down-sampling, channel equalization, HM-NPAM-4 symbol decision, and BER calculation. The OFDE method is considered as a channel equalization

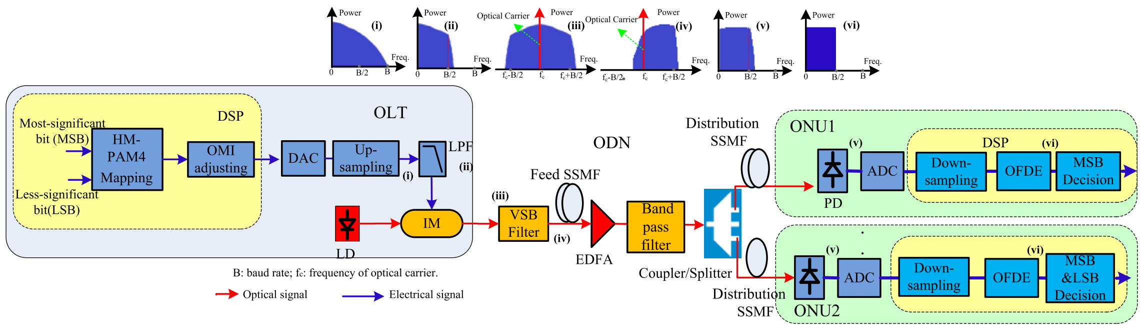

Fig. 1. The architecture of applying HM-NPAM-4 in IM/DD based TDM-PON.

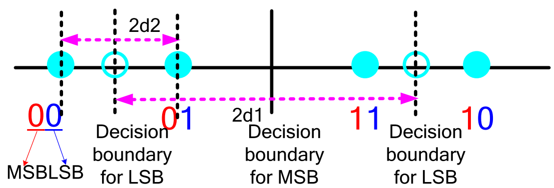

Fig. 2. The principle of HM-PAM-4.

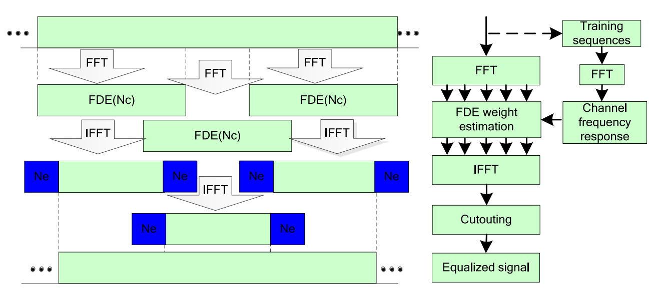

Fig. 3. The OFDE working principle diagram.

technology to mitigate ISI incurred by CD. Fig. 3 illustrates how OFDE equalizer works [43]. Specifically, first, the digital signal from ADC is segmented into a number of data blocks, which contains Nc data symbols. In order to form protection intervals among data blocks, N_e data symbols are added between two data blocks. After fast Fourier transform (FFT) operation, a frequency domain data block is multiplied by the equalizer's tap coefficient. The N_c symbols in a data block are transformed into the time domain by conducting the inverse FFT (IFFT) operation. Then, the N_e sampling points are removed from the corresponding equalized time domain signal, and the number of remaining valid data sampling points is $N_0 = N_c - 2N_e$. Finally, an HM-NPAM-4 symbol is demodulated by the related decision module. ONU-1 only has to demodulate MSB, which can be achieved by comparing the received signal to the decision boundary for MSB in Fig. 2. ONU-2 has to demodulate both MSB and LSB, and so the received signal has to be compared with the decision boundaries interactively. Note that the success of demodulating LSB depends on the hierarchical power ratio γ. As mentioned before, increasing γ reduces d_2 (which is the Euclidean distance between the constellation points in the actual PAM-4), thus increasing the BER of demodulating LSB.

Furthermore, for HM-NPAM-4 symbol decision, the decoder has to be able to adapt the threshold levels, which is represented by half of the symbol-level in the constellation. It means that the required received SNR for receiving the layer with higher protection level (MSB) requires a lower SNR than that of the less protected layer (LSB). Finally, it can be observed that the recovered shaped signal spectrum is half of the symbol rate in the conventional generated signal.

It is worth to note that the use of HM-NPAM-4 is only beneficial when different ONUs have different distances to their OLT, thus resulting in significant SNR margin. In the downstream communications, the OLT pairs its connected ONUs based on their SNR values. Thus, a lookup table can be formed for each search of the hierarchical power ratio by considering the system coverage area.

3. Simulation and results

In order to evaluate the performance of the HM-NPAM-4 in the IM/DD based TDM-PON system, we conduct extensive simulations in VPI transmission Maker v8.5 and Matlab. The performance of this scheme is analyzed. There are one OLT and two ONUs (i.e., ONU-1 and ONU-2, which are paired together to achieve HM-NPAM-4) in the IM/DD based TDM-PON system. The length of the feed fiber is 70 km, and the lengths of distribution fibers to ONU-1 and ONU-2 are 30 km and 10 km, respectively. Since ONU-1 is far away from the OLT, it only needs to demodulate the MSB in an HM-NPAM-4 symbol; meanwhile, ONU-2 is close to the OLT, and thus it needs to demodulate the LSB and MSB in an HM-NPAM-4 symbol. The other simulation parameters are list in Table 1. Note that an ONU can obtain the frequency response of a channel between an OLT and an ONU by using the training sequence (TS) method. That is, a training sequence is sent from the OLT to the ONU, which can acquire the frequency response of the channel by analyzing the received TS. Meanwhile, in the simulation setup, DAC/ADC quantization noise, laser line-width [52,53], and low-pass filtering effects are neglected. In addition, the optimized carrier-to-signal power ratio (CSPR) of the signal is adjusted by changing the OMI in the DSP. The digital signal is directly sent to a DAC, which converts the digital signal into the electrical signal. The electrical signal is then converted into the optical signal by an external electro absorption modulator (EAM), which is a type of optical intensity modulator. The optical signal is transmitted to a VSB filter, which we use Gaussian-shaped pass band, to mitigate the power fading. The received optical signal's power is adjusted by using a variable optical attenuator (VOA) to simulate the attenuation of an optical-power splitter. We consider the BER and ROP of an ONU as the system performance, and we will measure the system performance by varying various parameters, i.e. hierarchical power ratio γ, fiber length, and whether applying Nyquist pulse shaping and VSB filter or not. The BER threshold is set to be 3.8e−3, which can achieve 7% hard decision forward error correction (FEC) overhead limit.

3.1. Impact of hierarchical power ratio

We first evaluate how the hierarchical power ratio γ affects the system performance. Here, the SSMF fiber length is 100 km, and both LPF (which achieves Nyquist pulse shaping) and VSB filter are used in the system. Fig. 4 shows the BER and the ROP of ONU-1 (in demodulating the MSB and LSB in a HM-NPAM-4 symbol) with different values of γ. Note that the traditional non-hierarchical Nyquist

Table 1
The main simulation parameters and properties.

The simulation parameter	Value	The simulation parameter	Value
Modulation type	PAM-4	LD line width	1 MHz
Symbol rate	10 GB	LD output power	1 (mW)
FFT size	64 points	Overlap length	8 points
The Modulation index	0.5	Chirp factor	1.1
Number of PAM-4 symbol	100	The distance of ONUs and OLT	Variable
Number of PAM-4 training symbols	20	Cyclic prefix	1/8 symbol period
Nonlinear coefficient	2.6e−20	CD coefficient	16 (ps/nm· km)
Polarization mode dispersion coefficient	0.5e−12/31.62 (s/m$^{0.5}$)	Carrier frequency of OLT	193.1 (THz)
3-dB bandwidth of VSB filter	21.7G	Central frequency offset of VSB filter	11G
EDFA noise factor	4.5 (dB)	The sampling rate of each ONU	20 (GSa/s)
PIN noise factor	13e−12 (A/(Hz)$^{0.5}$)	The constellation distance (power)ratio	Variable

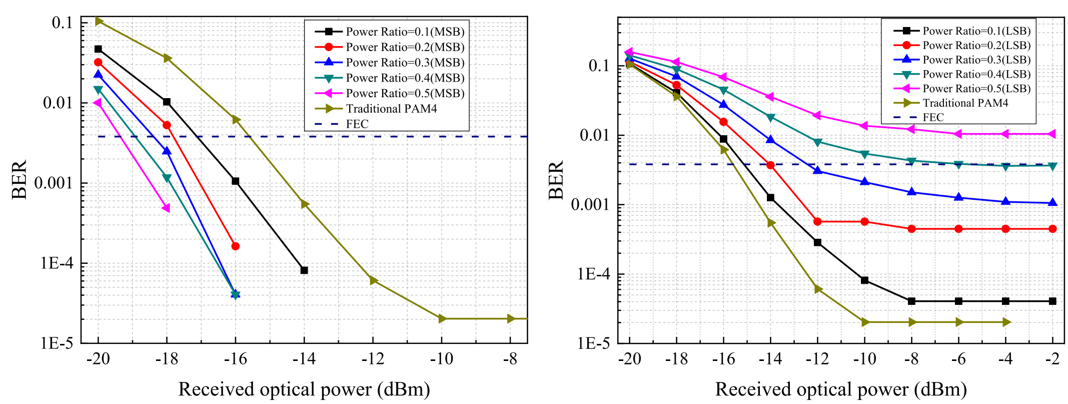

(a) MSB (b) LSB

Fig. 4. The measured BER and ROP (dBm) with different hierarchical power ratio of ONU-1.

pulsed PAM-4 (NPAM-4) is considered as the benchmark modulation. Also, the dotted line indicates the FEC threshold (i.e., BER threshold).

From Fig. 4(a), we can see that the receiver sensitivity of demodulating an N-PAM-4 symbol is −15.5 dBm, and the receiver sensitivities of demodulating the MSB in an HM-NPAM-4 symbol are −17 dBm, −17.8 dBm, −18.5 dBm, −18.9 dBm, and −19.6 dBm when γ are 0.1, 02, 0.3, 0.4 and 0.5, respectively. Thus, as compared to NPAM-4, applying HM-NPAM-4 can improve the sensitivity of demodulating the MSB in a symbol, and the receiver sensitivity is further improved as γ increases. Note that improving the sensitivity of MSB indicates that the ONU requires less ROP to satisfy the BER threshold (i.e., 3.8e−3). From Fig. 4(b), we can see that the receiver sensitivities of demodulating the LSB in an HM-NPAM-4 symbol become −14.8 dBm, −14 dBm, −12.2 dBm, and −6 dBm when γ are 0.1, 0.2, 0.3, and 0.4, respectively. Note that when $\gamma = 0.5$, the receiver sensitivity of demodulating the LSB is not valid since the BER is always larger than the BER threshold. Thus, as compared to NPAM-4, applying HM-NPAM-4 reduces the sensitivity of demodulating the LSB in a symbol, and the sensitivity of LSB is further reduced as γ increases. Therefore, differential power budgets of 1.7 dB, 2.8 dB, 6.3 dB and 12.9 dB between the MSB and LSB can be obtained when γ are 0.1, 0.2, 0.3, and 0.4, respectively. Therefore, for this TDM-PON system with two ONUs, the support differential sensitivity can be converted to the required ROPs of ONUs with different link conditions. That is, if we consider the path loss of 0.2 dB/km, the differential reach for the two ONUs are 8.5 km, 14 km, 31.5 km and 64.5 km, respectively.

Fig. 5 shows the eye diagram and the histogram of ONU-1 based on traditional NPAM-4 and HM-NPAN-4 when $\gamma = 0.3$ and the ROP is −12 dBm.

As observed in Fig. 5(a), the results of measured eye diagram show that the traditional NPAM-4 format has standard equal distances between its modulation levels. In addition, the separate detection of the NPAM-4 signal is distributed on $-3, -1, +1,$ and $+3$ constellation level, as shown in Fig. 5(c). However, as shown in Fig. 5(b), HM-NPAM-4 exhibits the unequal signal level spacing in the eye diagram. In this case, the vertical eye of LSB incurs a smaller closure penalty. The inner eye of the HM-NPAM-4 scheme is similar with that of the OOK scheme. Accordingly, the received HM-NPAM-4 symbol is distributed on $-3, -1.6, +1.6,$ and $+3$ constellation levels. In addition, a larger deviation of the MBS's constellation level in the HM-NPAM-4 histogram diagram can be shown in Fig. 5(d). Thus, the results in Fig. 5 are consistent with the previous description with respect to Fig. 2.

3.2. Impact of fiber transmission distance

In this section, we will evaluate how the fiber transmission distance between the OLT and its ONUs affects the system performance when γ equals 0.2 and 0.4.

Fig. 6 shows the BER and ROP of ONU-1 and ONU-2. We can see that the receiver sensitivities of ONU-1 for demodulating the MSB are −17.8 dBm and −18.85 dBm when γ equals 0.2 and 0.4, respectively. Similarly, the receiver sensitivities of ONU-2 for demodulating the MSB are −18 dBm and −19.4 dBm when γ equals 0.2 and 0.4, respectively. Meanwhile, the receiver sensitivities of ONU-2 for demodulating the LSB are −14.8 dBm and −12 dBm when γ equals 0.2 and 0.4, respectively. Thus, we can conclude that at the certain γ, for MSB demodulating, the receiver sensitivity of ONU-2 (higher SNR) is better than the ONU-1(lower SNR). This is because an ONU incurs less impairment as the transmission distance between the OLT and the ONU decreases. In addition, we can see that the MSB has more dispersion tolerance than the LSB.

On the other hand, when γ equals to 0.2 and 0.4, the differential power budgets between the 70 km feed fiber transmission and ONU-1 are 5.75 dB and 2.3 dB, respectively. Meanwhile, the difference of the power budgets between the 70 km feed fiber transmission and ONU-2 are 6.1 dB and 2.5 dB, respectively. Therefore, the redistribution of power margin can be obtained for different γ. For instance, owing to

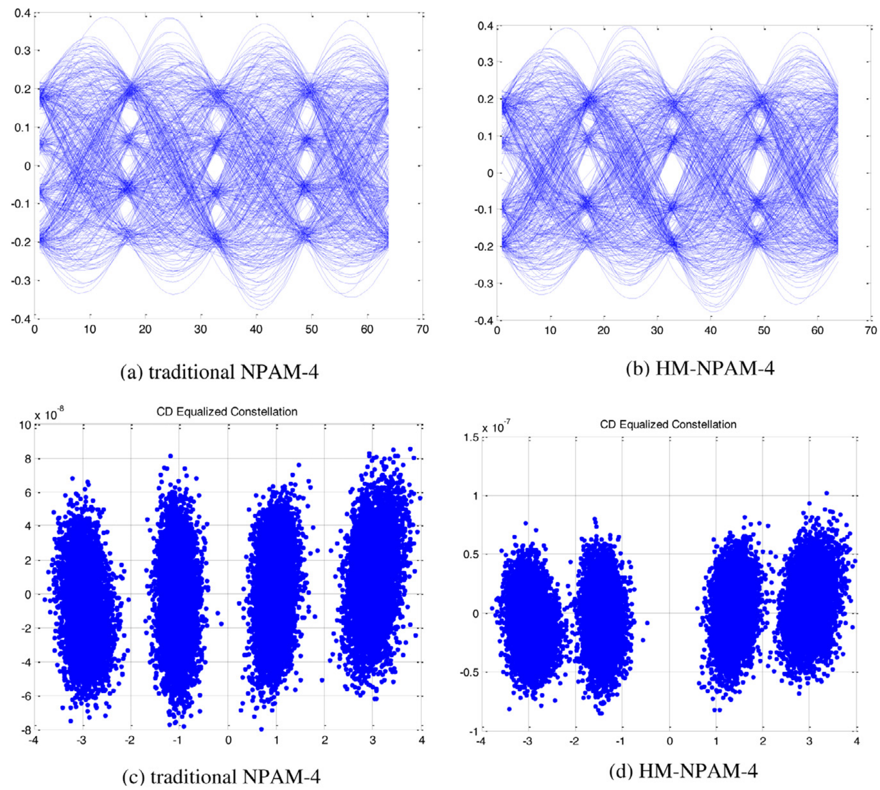

Fig. 5. The eye diagram (a) (b) and histogram of the samples (c) (d) of ONU-1 for traditional NPAM-4 and HM-NPAM-4 at −12 dBm ROP.

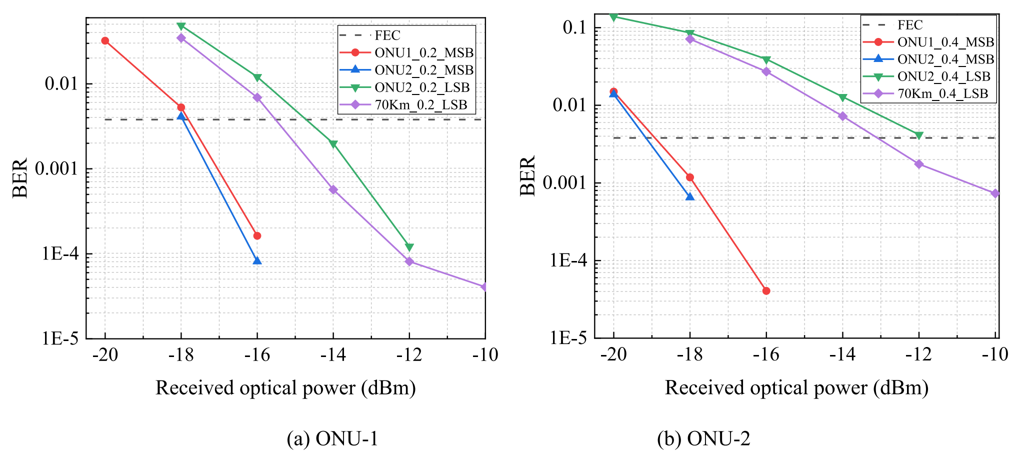

Fig. 6. The measured BER and ROP (dBm) of ONU-1 and ONU-2.

the difference of SNR between ONU-1 and ONU-2 (which is caused by the 20 km fiber transmission distance), γ can be equal to 0.3 in order to optimize the power margin redistribution. Moreover, if the distance between the OLT and ONU-1 needed to be increased for longer reach, the γ can be increased to achieve better receiver sensitivity for ONU-1 in demodulating the MSB. That is, we can find that adjusting hierarchical power ratio γ by applying HM-NPAM-4 in the IM/DD based TDM-PON system can dynamical modify the power margin (i.e., ROP-receiver sensitivity) of the ONUs.

3.3. Impact of nyquist pulse shaping

In this section, we investigate the BER and ROP of ONU-1 and ONU-2 based on HM-NPAM-4 with and without an LPF (Nyquist pulse-shaping) when $\gamma = 0.3$.

As shown in Fig. 7, compared to the without Nyquist pulse-shaping case, we can see that the receiver sensitivity of ONU-1 for demodulating the MSB in an HM-NPAM-4 symbol is improved by 0.18 dB with Nyquist pulse-shaping. Meanwhile, the receiver sensitivity of ONU-2 for demodulating the MSB in an HM-NPAM-4 symbol with Nyquist pulse-shaping, has the slightly improvement. Thus, due to the channel equalization, the receiver sensitivities of the ONUs in the MSB demodulation case have less impacts of distortion.

In addition, the receiver sensitivity of ONU-2 for demodulating the LSB is better than receiver sensitivity of ONU-1. Besides, the receiver sensitivities of both ONUs have significant improvement with Nyquist pulse-shaping as compared to that without Nyquist pulse-shaping. When the LPF filter is not utilized, the receiver sensitivities of both ONUs are not valid since the BERs are always larger than the BER threshold. The reason of the above results can be explained

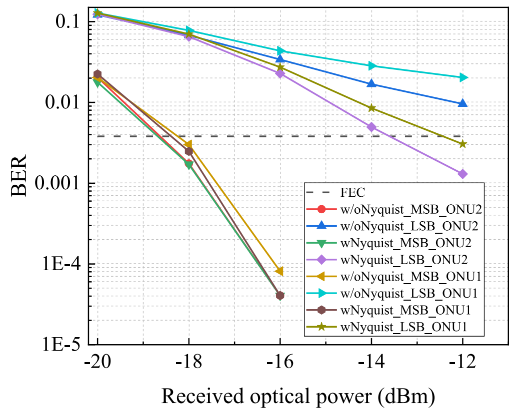

Fig. 7. The measured BER and ROP (dBm) of ONU-1 and ONU-2 with or without Nyquist pulse-shaping.

as follows. Although the linear ISI can be reduced by OFDE, applying Nyquist pulse-shaped filter can further reduce the ISI because a wider bandwidth of a link incurs a stronger ISI and the bandwidth is reduced by half if the Nyquist pulse-shaped filter is utilized. Therefore, applying Nyquist pulse-shaped filter can effectively enhance the system performance by reducing the ISI. Moreover, as compared to the MSB demodulation case, no matter the Nyquist pulse-shaped filter is utilized, the sensitivity of ONU-1 or ONU-2 in demodulating LSB is much worse.

3.4. Impact of vsb filter

Finally, we compare the system performance based on HM-NPAM-4 with and without VSB filter, when $\gamma = 0.3$ and ROP is -12 dBm. Fig. 8(a) and Fig. 8(b) show the electrical spectrum of ONU-1 after PD with and without VSB filter, respectively.

From the figures we can see that, when the VSB filter is not utilized, there is a dip incurred by power fading in ONU-1 over the frequency. Note that the power fading can reduce the available system bandwidth. On the contrary, we can obtain the flat channel frequency response, which indicates a low power fading in ONU-1 by implementing the VSB filter. Thus, we conclude that applying VSB filter in HM-NPAM-4can reduce power fading, thus increasing transmission distance between the OLT and the ONU. Fig. 9(a) shows the BER and ROP of ONU-1 with and without the VSB filter when $\gamma = 0.3$. From the figure, we can see that the BER cannot meet the desired BER threshold when VSB filter is not utilized. On the contrary, a large improvement on BER performance can be obtained when the VSB filter is utilized. In addition, the receiver sensitivity of ONU-1 in demodulating MSB is improved by 5.8 as compared to that in demodulating LSB.

Moreover, Fig. 9(b) shows the measured BER and ROP over different SSMF transmission. From the figure, we can find a critical transmission distance, i.e., 50 km, in which a VSB filter has to be utilized in order to satisfy the BER threshold. That is, as long as the distance between an OLT and an ONU is longer than 50 km, it is necessary to utilize a VSB filter to achieve the desired receiver sensitivity.

4. Conclusions

In this paper, an efficient HM-NPAM-4 scheme by utilizing hybrid equalization (i.e., VSB filter and OFDE) is proposed to fully utilize the available power margin. Furthermore, we present the designs and numerical simulations of applying HM-NPAM-4 in IM/DD based TDM-PON system. The simulation results demonstrate that the hierarchical power ratio can be adjusted according to the corresponding SNR of the ONU in order to optimize the power margin. In addition, the OFDE and VSB filter are demonstrated to mitigate the linear ISI and power fading in HM-NPAM-4. In the future, we will investigate on how to optimize the hierarchical power ratio and mitigate nonlinear signal-to-signal beating interference (SSBI) distortion incurred by square-law detection in the HM-NPAM-4 scheme.

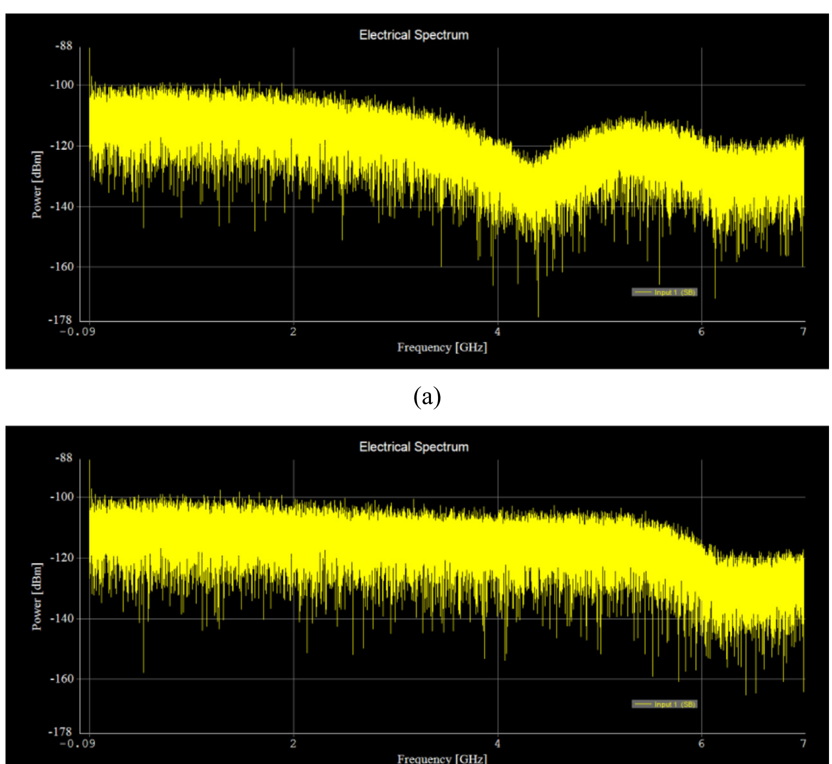

(b)

Fig. 8. The measured electrical spectrum performance of ONU-1 (a) without VSB filter (b) with VSB filter.

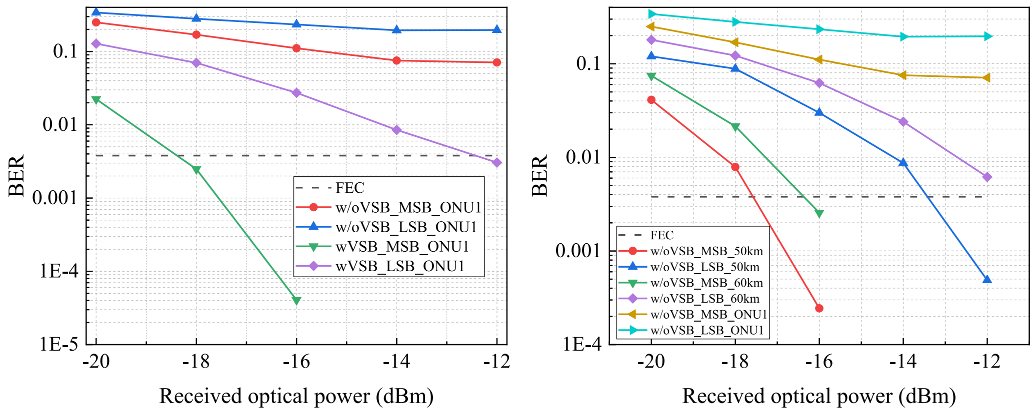

(a) ONU-1 with and without VSB filter (b) different SSMF transmission without VSB filter

Fig. 9. The measured BER and ROP (dBm) with/without VSB filter.

Funding

This work was supported in part by the National Science Foundation under Award No. OIA-1757207 and National Natural Science Foundation of China under Award No. 61801043.

References

[1] P.E. Green, Fiber to the Home—the New Empowerment, Wiley, New York, 2006.

[2] V. Kachhatiya, S. Prince, Downstream performance analysis and optimization of the next generation passive optical network stage 2 (NG-pon2), Opt. Laser Technol. 104 (2018) 90–102.

[3] D.V. Veen, V. Houtsma, Symmetrical 25 Gbps TDM-PON with 315 dB optical power budget using only off-the-shelf 10 Gbps optical components, J. Lightwave Technol. (2016) 1636–1642.

[4] S. Zhou, L. Xiang, F. Effenberger, et al., Low-latency high-efficiency mobile fronthaul with TDM-PON (mobile-PON), J. Opt. Commun. Netw. 10 (1) (2018) A20–A26.

[5] S. Yin, D.V. Veen, V. Houtsma, et al., Investigation of symmetrical optical amplified 40 Gbps PAM-4/Duobinary TDM-PON using 10G optics and DSP, in: Proc. Opt. Fiber Commun. Conf. Exhib., OFC, 2016, pp. 1–3.

[6] J. Wei, N. Eiselt, H. Griesser, et al., Demonstration of the first real-time end-to-end 40-Gb/s PAM-4 for next-generation access applications using 10-Gb/s transmitter, J. Lightwave Technol. 34 (7) (2016) 1628–1635.

[7] B.H. Zhang, S. Fu, J. Man, et al., 30 Km downstream transmission using 4 × 25 Gb/s 4-PAM modulation with commercial 10 Gbps TOSA and ROSA for 100 Gb/s-PON, in: Proc. Opt. Fiber Commun. Conf. Exhib., OFC, 2014, pp. 1–3.

[8] J. Gao, N. Cheng, H. Zhang, Demonstration of the first 29dB power budget of 25-Gb/s 4-PAM system without optical amplifier for next generation access network, in: Proc. Opt. Fiber Commun. Conf. Exhib., OFC, 2016, pp. 1–3.

[9] M.G. Saber, M.O. Mohamed, H. Michael, et al., DSP-free 25 Gbit/s PAM-4 transmission using 10 G transmitter and coherent amplification, IEEE Photonics Technol. Lett. 30 (17) (2018) 1547–1550.

[10] S. Barthomeuf, F. Saliou, L.A. Neto, et al., Real-time downstream 25Gbit/s PAM4 for high speed TDM-PONs with both 25 and 12.5Gbit/s ONUs, in: Proc. Opt. Fiber Commun. Conf. Exhib., OFC, 2018, pp. 1–3.

[11] K. Zhang, Q. Zhuge, H. Xin, et al., Demonstration of 50Gb/sλ symmetric PAM4 TDM-PON with 10G-class optics and DSP-free ONUs in the O-band, in: Proc. Opt. Fiber Commun. Conf. Exhib., OFC, 2018, pp. 1–3.

[12] J.D. Reis, A. Shahpari, R. Ferreira, et al., Performance optimization of Nyquist signaling for spectrally efficient optical access networks [invited], J. Opt. Commun. Netw. 7 (2) (2015) A200–A208.

[13] N. Eiselt, D. Muench, A. Dochhan, et al., Performance comparison of 112-Gb/s DMT, nyquist PAM-4, and partial-response PAM-4 for future 5G ethernet-based fronthaul architecture, J. Lightwave Technol. 99 (2018) 1807–1814.

[14] M. Nakamura, F. Hamaoka, A. Matsushita, et al., Advanced DSP technologies with symbol-rate over 100-Gbaud for high-capacity optical transport network, in: Proc. Opt. Fiber Commun. Conf. Exhib., OFC, 2018, pp. 1–3.

[15] N. Kikuchi, R. Hirai, Intensity-modulated / direct-detection (IM/DD) Nyquist pulse-amplitude modulation (PAM) signaling for 100-Gbit/s/λ optical short-reach transmission, in: Proc. European Conference on Optical Communication, 2014, pp. 1–3.

[16] M. Morimoto, H. Harada, M. Okada, et al., A study on power assignment of hierarchical modulation schemes for digital broadcasting, IEICE Trans. Commun. 77 (12) (1994) 495–1500.

[17] C.S. Hwang, Y. Kim, An adaptive modulation method for multicast communications of hierarchical data in wireless networks, in: Proc. IEEE International Conference on Communications, ICC, vol. 2, 2002, pp. 896–900.

[18] N. Shibata, N. Iiyama, J.I. Kani, et al., Star-QAM constellation design for hierarchically modulated PON systems with 20-Gbps PSK and 10-Gbps OOK signals, J. Lightwave Technol. 32 (18) (2014) 3184–3191.

[19] N. Shibata, J. Kani, Constellation design for next-generation hierarchically-modulated PON systems, in: Proc. in Proc. Broadband Access Communication Technologies, vol. VII, 2013, pp. 1–3.

[20] N. Iiyama, J.I. Kani, J. Terada, et al., Demonstration of hierarchical star 8-QAM designed for coexistence of 10 G-EPON and DSP-based PON with 30-dB loss budget, in: Proc. Optoelectronics & Communications Conference held Jointly with International Conference on Photonics in Switching, IEEE, 2013, pp. 1–3.

[21] N. Yoshimoto, J. Kani, S.Y. Kim, et al., DSP-based optical access approaches for enhancing NG-PON2 systems, IEEE Commun. Mag. 51 (3) (2013) 58–64.

[22] P. Cao, X. Hu, Z. Zhuang, et al., Power margin improvement for OFDMA-PON using hierarchical modulation, Opt. Express 21 (7) (2013) 8261–8268.

[23] M.D. Santa, C. Antony, G. Talli, et al., Power budget improvement in passive optical networks using PAM-4 hierarchical modulation, IEEE Photonics Technol. Lett. (99) (2017) 1747–1750.

[24] R. van der Linden, N.C. Tran, E. Tangdiongga, et al., Improvement on received optical power based flexible modulation in a PON by the use of non-uniform PAM, in: Proc.Optical Communication, ECOC, European Conference on, 2017, pp. 1–3.

[25] R. van der Linden, N.C. Tran, E. Tangdiongga, et al., Utilizing unused power budget to increase network capacity in practical PON deployments by introducing flexible modulation, in: Proc. European Conference on Optical Communication 2015, pp. 1–4.

[26] R. van der Linden, N.C. Tran, E. Tangdiongga, et al., Optimization of flexible non-uniform multi-level PAM for maximizing the aggregated capacity in PON deployments, J. Lightwave Technol. 36 (12) (2018) 2328–2336.

[27] R. van der Linden, N.C. Tran, E. Tangdiongga, et al., Increasing flexibility and capacity in real PON deployments by using 2/4/8-PAM formats, J. Opt. Commun. Netw. 9 (1) (2017) A1–A8.

[28] D.V. Veen, V. Houtsma, H. Chow, Demonstration of symmetrical 25 Gbps quaternary PAM/duobinary TDM-PON with multilevel interleaving of users, in: Proc.European Conference on Optical Communication, 2015, pp. 1–4.

[29] R. van der Linden, N.C. Tran, E. Tangdiongga, et al., Optimization of flexible non-uniform multilevel PAM for maximizing the aggregated capacity in PON deployments, J. Lightwave Technol. 36 (12) (2018) 2328–2336.

[30] J. Zhang, J.S. Wey, J. Shi, et al., Experimental demonstration of unequally spaced PAM-4 signal to improve receiver sensitivity for 50-Gbps PON with power-dependent noise distribution, in: Proc. Opt. Fiber Commun. Conf. Exhib., OFC, 2018, pp. 1–3.

[31] R. van der Linden, Adaptive Modulation Techniques for Passive Optical Networks, Technische Universiteit Eindhoven, 2018.

[32] L. Chen, F. Halabi, P. Roger Giddings, J.M. Tang, Subcarrier index-power modulated optical OFDM with superposition multiplexing for IMDD transmission systems, J. Lightwave Technol. 34 (22) (2016) 5284–5292.

[33] J.A. Altabas, S. Rommel, R. Puerta, et al., Non-orthogonal multiple access and carrierless amplitude phase modulation for 5G mobile networks, in: Proc. European Conference on Optical Communication, 2017, pp. 1–4.

[34] B. Lin, K. Zhang, Y. Tian, et al., Experimental demonstration of an NOMA scheme for passive optical network, in: Asia Communications and Photonics Conference, Optical Society of America, 2017, pp. 1–3, Su2A. 30.

[35] B. Lin, Z. Ghassemlooy, X. Tang, et al., Experimental demonstration of an NOMA-PON with single carrier transmission, Opt. Commun. (396) (2017) 66–70.

[36] B. Lin, K. Zhang, X. Tang, et al., Optical MIMO NOMA-PON based on single carrier transmission and polarization interleaving, Opt. Fiber Technol. 36 (2017) 412–416.
[37] J.A. Altabas, S. Rommel, R. Puerta, et al., Non-orthogonal multiple access and carrierless amplitude phase modulation for 5G mobile networks, in: Proc. European Conference on Optical Communication, 2017, pp. 1–4.
[38] J.A. Altabas, S. Rommel, R. Puerta, et al., Non-orthogonal multiple access and carrierless amplitude phase modulation for flexible multi-user provisioning in 5G mobile networks, J. Lightwave Technol. (99) (2017) 5456–5463.
[39] N. Kikuchi, R. Hirai, T. Fukui, Quasi single-sideband (SSB) IM/DD Nyquist PAM signaling for high-spectral efficiency DWDM transmission, in: Proc. Opt. Fiber Commun. Conf. Exhib., OFC, Th2A.41, 2016, pp. 1–3.
[40] R. Deng, J. He, J. Yu, et al., Experimental demonstration of 20-Gb/s dual-band Nyquist PAM-4 transmission over a short-reach IM/DD system using super-Nyquist sampling technique, Opt. Lett. 43 (11) (2018) 2640–2643.
[41] H. Yamazaki, M. Nagatani, S. Kanazawa, et al., 160-Gbps Nyquist PAM-4 transmitter using a digital-preprocessed analog-multiplexed DAC, in: Proc. European Conference on Optical Communication, 2015, pp. 1–3.
[42] N. Liu, X. Chen, C. Ju, et al., Nyquist 4-ary pulse amplitude modulation scheme based on electrical Nyquist pulse shaping and fiber Bragg grating filter, Opt. Engine 54 (4) (2015) 046105.
[43] C. Ju, N. Liu, Iterative nonlinear ISI cancellation in optical tilted filter-based Nyquist 4-PAM system, Opt. Fiber Technol. 31 (2016) 42–46.
[44] J.J. Shynk, Frequency-domain and multirate adaptive filtering, IEEE Signal Process. Mag. 9 (1) (1992) 14–37.
[45] M.S. Faruk, S.J. Savory, Digital signal processing for coherent transceivers employing multilevel formats, J. Lightwave Technol. 35 (5) (2017) 1125–1141.
[46] J. He, H. Dong, R. Deng, et al., Enhanced performance of CAP system using an overlap frequency-domain equalization scheme, IEEE Photon. J. 8 (2) (2016) 1–8.
[47] H.Y. Chen, J. Lee, N. Kaneda, et al., Comparison of VSB PAM-4 and OOK signal in an EML-based 80-km transmission system, IEEE Photonics Technol. Lett. 29 (23) (2017) 2063–2066.
[48] Z. Zhang, Q. Guo, C. Ju, et al., Optical- and electrical-domain compensation techniques for next-generation passive optical networks, IEEE Commun. Mag. 57 (4) (2019) 144–150.
[49] J. Zhang, J. Yu, X. Li, et al., 100 Gbit/s VSB-PAM-n IM/DD transmission system based on 10 GHz DML with optical filtering and joint nonlinear equalization, Opt. Express 27 (5) (2019) 6098–6105.
[50] Z. Xing, D. Patel, T.M. Hoang, 100Gb/s 16-QAM transmission over 80 km SSMF using a silicon photonic modulator enabled VSB-IM/DD system, in: Proc. Opt. Fiber Commun. Conf. Exhib., OFC, 2018, pp. 1–3.
[51] P.K. Vitthaladevuni, M.S. Alouini, A recursive algorithm for the exact BER computation of generalized hierarchical QAM constellations, IEEE Trans. Inf. Theory 49 (1) (2003) 297–307.
[52] A. Yekani, L.A. Rusch, Interplay of bit rate, linewidth, bandwidth, and reach on optical DMT and PAM with IMDD, IEEE Trans. Commun. (99) (2019) 2908–2913.
[53] A. Yekani, S. Amiralizadeh, L.A. Rusch, Analytical study of optical SSB-DMT with IMDD, J. Lightwave Technol. 36 (3) (2018) 666–674.